

\bar{p} - p CROSS SECTIONS FROM 534 TO 1068 Mev

T. Elioff, L. Agnew, O. Chamberlain, H. Steiner, C. Wiegand, and T. Ypsilantis
Lawrence Radiation Laboratory, University of California, Berkeley, California
(Received August 26, 1959)

We report here measurements of the antiproton-proton, elastic, inelastic, and charge-exchange cross sections for antiproton energies of 534, 700, 816, 948, and 1068 Mev. The total cross section remains large with respect to nucleon-nucleon cross sections in the same energy range. It has not yet been possible to determine precisely what fraction of the inelastic cross section is due to annihilation.

The antiproton beam was formed in a manner similar to that of previous experiments.^{1,2} A schematic diagram of the experimental area is presented in Fig. 1, and Table I identifies the principal components. The 6-Bev internal proton beam of the Bevatron impinged on a carbon or polyethylene target at one of three different target positions schematically represented by T . Choice of the proper target enabled our mass spectrograph to select antiprotons within the desired energy range at angles from 0° to 5° (lab) with respect to the direction of the incident proton beam. The ratio of antiprotons to other negative particles (mostly pions) transmitted through the spectrograph was about 1/20 000 for the highest antiproton energies.

The antiprotons were distinguished from other particles in the beam by their time of flight between the scintillation counters S_1 , S_2 , and S_3 in coincidence with a count from the antiproton velocity-selecting Čerenkov counter, VSC II. In addition it was required that the meson Čerenkov

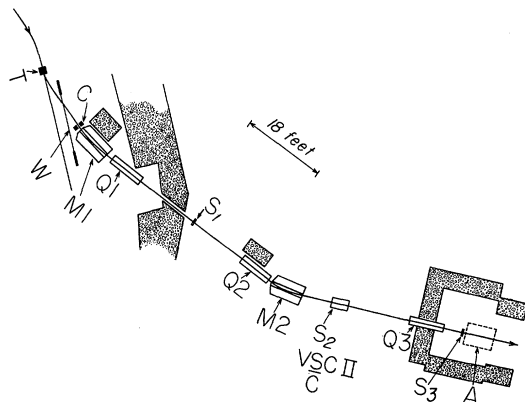


FIG. 1. Schematic view of the Bevatron experimental area. See Table I.

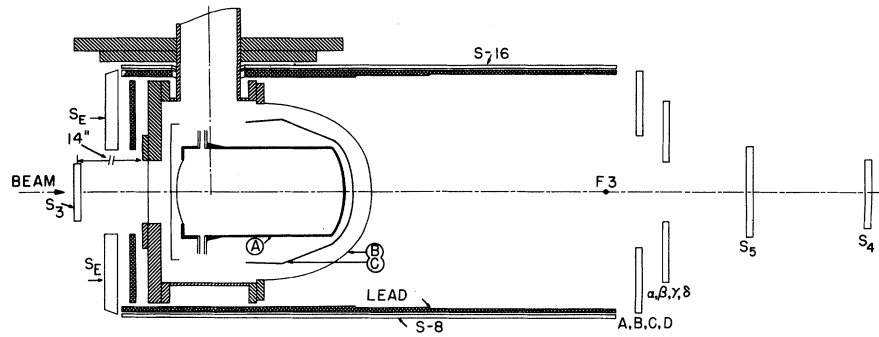
counter, \bar{C} , did not count. The ratio of pions counted accidentally to pions transmitted through the system was less than 10^{-7} .

Identified antiprotons which traversed the magnetic channel entered a target positioned immediately behind S_3 . This target could be filled with either liquid hydrogen or deuterium and was completely surrounded by an array of scintillation counters. Figure 2 displays a side view of the target and counter system. Figure 3 shows the counter system from the beam-exit end. Counters S_4 and S_5 detected the transmitted antiprotons. The other 25 counters detected either a scattered antiproton or the products from inelastic antiproton-proton collisions. The coincidence counts between the incident antiproton and the 27 counters were displayed on an oscilloscope and photo-

Table I. Experimental components of Fig. 1.

Symbol	Component description
T	Bevatron target area
W	Thin window of Bevatron vacuum system
C	Brass collimator 6-in. diam by 8 in. thick
$M1, M2$	60 in. long deflection magnets with 12- by 7-in. aperture; $\theta_{M1} = 17^\circ$, $\theta_{M2} = 25^\circ$
$Q1, Q2, Q3$	Sets of quadrupole focusing magnets of 8-in. aperture
S_1	Plastic scintillation counter $3\frac{1}{2}$ -in. diam by $\frac{1}{4}$ in. thick
S_2	Plastic scintillation counter $3\frac{1}{16}$ -in. diam by $\frac{1}{4}$ in. thick
VSC II	Antiproton narrow-band velocity-selecting Čerenkov counter which utilizes a cyclohexene ($n = 1.46$, $\rho = 0.8$) radiator $3\frac{1}{4}$ -in. diam and 4.7 in. long. The velocity resolution is $\Delta\beta = 0.03$ in the range $0.95 > \beta > 0.70$
\bar{C}	Meson Čerenkov counter which utilizes the same radiator as VSC II but views only Čerenkov light that is totally internally reflected, i. e., for $\beta > 0.95$
S_3	Plastic scintillation counter 5-in. diam by $\frac{3}{8}$ in. thick
A	Area for H_2 target and final counter system

FIG. 2. Side view of target and counter system. For clarity, the figure is not shown precisely to scale. The container A which could be filled with liquid hydrogen or deuterium is a stainless steel cylinder 12 in. long and 6 in. in diameter with 0.008-in. walls except for the beam entrance wall which is 0.010-in. Mylar. Sixteen scintillation counters, S-1 through S-16, cylindrically surround the container A. Each has dimensions 38 by 4.1 by 0.375 in. Scintillators S_E , A, B, C, D, α , β , γ , δ , S_4 , and S_5 are shown more explicitly in the next figure. The lead between the target and the scintillators is removable. The heat shield C is 0.003-in. copper; B is a thin region of the vacuum wall which is 0.035-in. aluminum.



graphed whenever an antiproton entered the target.

The pulses photographed on the oscilloscope film were classified as follows:

- (a) If S_4 and S_5 counted or if S_5 counted alone, the antiproton did not interact.
- (b) Elastic scattering occurred if a single count was detected in one of the counter rings (see Fig. 3) or in counters S-1 through S-16 around the target. For scattering angles greater than 15° in the laboratory system, the recoil proton was also observable.
- (c) Inelastic scattering or annihilation occurred when any three or more counters registered or when two counters registered and the kinematics were not consistent with elastic scattering.
- (d) A charge-exchange collision occurred when none of the counters registered.

The analysis of 70% of the film data has yielded the cross sections shown in Table II. These cross sections include small corrections for accidentals caused by neutron background in the Bevatron area, annihilations in counters, and the escape of particles through small spaces between

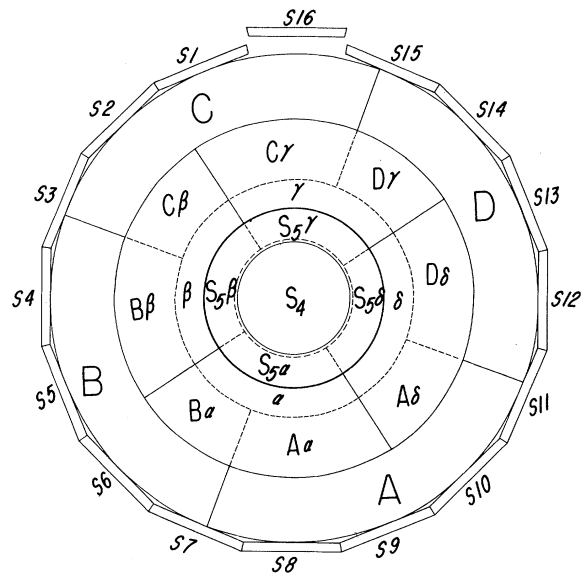


FIG. 3. Schematic view from the beam-exit end of the counter system, which displays counters A, B, C, D, α , β , γ , δ , S_4 , and S_5 and their overlapping regions as well as an end view of counters S-1 through S-16.

Table II. \bar{p} - p cross sections at various energies.

\bar{p} energy (Mev)	\bar{p} - p cross section (mb)			
	Total	Elastic	Inelastic	Charge exchange
534 ± 25	119 ± 6	44 ± 6	69 ± 5	6 ± 2
700 ± 33	114 ± 5	43 ± 5	64 ± 4	8 ± 2
816 ± 37	105 ± 6	37 ± 5	60 ± 5	7 ± 2
948 ± 42	96 ± 3	33 ± 3	56 ± 3	8 ± 2
1068 ± 46	96 ± 4	30 ± 3	58 ± 3	7 ± 1

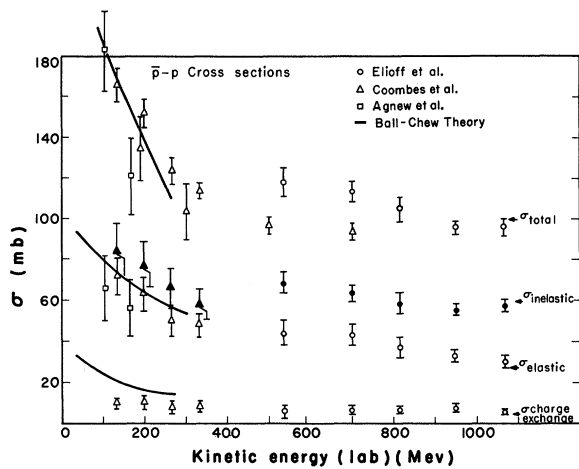


FIG. 4. Antiproton-proton total, elastic, inelastic, and charge-exchange cross sections as a function of antiproton laboratory kinetic energy. The round points are the results of this experiment. The triangular points are from reference 5 and reference 3. The square points are from reference 4. For clarity the inelastic points are darkened.

counters. In the case of the total and the elastic cross sections, an experimental correction has been made to include forward scattering by extrapolating total cross-section measurements at small cutoff angles to zero solid angle.

Figure 4 shows the cross sections given by this experiment and, for comparison, the results of previous experiments.³⁻⁵

In order to obtain assurance that our system could reproduce known cross sections, a positive proton beam was sent through our apparatus. This was done by scattering a 1.2-Bev internal Bevatron beam from a fourth target positioned near the region *T* of Fig. 1. We obtained the proton-proton cross sections at 2 energies and the results are tabulated in Table III. Precise

agreement was obtained with the results of other experiments.^{6,7}

The new antiproton results presented here agree reasonably well with the results of a previous experiment at 457 Mev.⁸ An apparent paradox drawn from the information of two prior experiments^{8,5} seems to be nonexistent. The somewhat incomplete prior data (incomplete in the sense that the elastic-scattering cross section was never measured) indicated a very large absorption cross section with little or no diffraction scattering—a phenomenon that is difficult to explain.⁹ A clarification of the situation can best be seen by the comparisons of Table IV.

The results of this experiment should be more reliable than those of the previous experiments as a more efficient means of distinguishing annihilation events was used and simultaneous measurements of the total, elastic, and charge exchange cross sections could be made. The total cross sections of reference 5 are consistently low compared to later measurements by the same authors at lower energies³ (see Fig. 4). The H₂O-D₂O-O₂ subtraction procedure of reference 8 inherently limits the accuracy of their results. Thus we conclude from Table IV that the value of the total cross section at 500 Mev⁵ is probably 20 mb too low and the inelastic cross section at 457 Mev⁸ is perhaps 20 mb too high.

From the 534-Mev data, one observes that more than half of the scattering is strongly

Table III. $p^+ - p$ cross sections for two energies.

p^+ energy (Mev)	$p^+ - p$ cross sections (mb)		
	Total	Elastic	Inelastic
528	30 ± 7	24 ± 5	6 ± 3
940	49 ± 5	26 ± 3	23 ± 3

Table IV. Comparison of $\bar{p} - p$ cross sections near 500 Mev.

Experiment	$\bar{p} - p$ cross sections (mb)				
	Total (0°)	Total (14°)	Inelastic	Elastic	Charge exchange
Chamberlain <i>et al.</i> ^a (457 Mev)		104 ± 8	89 ± 7
Cork <i>et al.</i> ^b (500 Mev)	97 ± 4
This experiment (534 Mev)	119 ± 6	93 ± 6	69 ± 5	44 ± 6	6 ± 2

^aSee reference 8.

^bSee reference 5.

peaked forward within a 14° laboratory angle. The latest results also indicate that the total elastic-scattering cross section constitutes $\sim 1/3$ of the total cross section in the energy range we have measured. This ratio has been indicated by a phenomenological black-sphere model of Koba and Takeda for a sphere radius of $\sim \frac{2}{3}\hbar/m_\pi c$.¹⁰

It is surprising that the inelastic cross section does not decrease appreciably with increasing energy which may indicate a longer-range annihilation interaction than expected.⁹ The Ball-Chew theory,¹¹ which is in agreement with the low-energy antiproton data, attributes the annihilation interaction to a rather short-range absorbing core. Of course the inelastic cross section as presented here includes both annihilation and meson production. From the partial analysis of the 948-Mev inelastic events, it appears that not more than about 10 mb of the inelastic cross section can be due to meson production. (The remaining 46 mb must then be attributed to annihilation.) This analysis is based on the assumption that production of 2 or more mesons is negligible except in annihilation. The assumption seems warranted because double meson production is known to be very small in nucleon-nucleon collisions at this energy.^{7,12,13}

Upon completion of our analysis we hope to discuss more fully the inelastic process. In addition to the antiproton-proton cross sections, we have the antiproton-deuteron cross sections at the same five energies. These results will be presented in a later publication.

We are grateful to Professor Emilio Segrè for his interest and advice during the initial stages of the experiment. We thank Dr. Richard Lander, Dr. Norman Booth, and Dr. Jan Button for their help during the course of the experiment.

¹Chamberlain, Segrè, Wiegand, and Ypsilantis, *Phys. Rev.* **100**, 947 (1955).

²Agnew, Chamberlain, Keller, Mermod, Rogers, Steiner, and Wiegand, *Phys. Rev.* **108**, 1545 (1957).

³Coombes, Cork, Galbraith, Lambertson, and Wenzel, *Phys. Rev.* **112**, 1303 (1958).

⁴Agnew, Elioff, Fowler, Gilly, Lander, Oswald, Powell, Segrè, Steiner, White, Wiegand, and Ypsilantis, University of California Radiation Laboratory Report UCRL-8822, June, 1959 (unpublished).

⁵Cork, Lambertson, Piccioni, and Wenzel, *Phys. Rev.* **107**, 248 (1957).

⁶References D11, B5, and S1 in W. Hess, *Revs. Modern Phys.* **30**, 368 (1958).

⁷Batson, Culwick, Clepp, and Riddiford, in 1958 International Conference on High-Energy Physics at CERN, edited by B. Ferretti (CERN, Scientific Information Service, Geneva, 1958), p. 74.

⁸Chamberlain, Keller, Mermod, Segrè, Steiner, and Ypsilantis, *Phys. Rev.* **108**, 1533 (1957).

⁹1958 International Conference on High-Energy Physics at CERN, edited by B. Ferretti (CERN, Scientific Information Service, Geneva, 1958), pp. 107, 108.

¹⁰Z. Koba and G. Takeda, *Progr. Theoret. Phys.* (Kyoto) **19**, 269 (1958).

¹¹J. Ball and G. Chew, *Phys. Rev.* **109**, 1395 (1958).

¹²Fowler, Shutt, Thorndike, Whittemore, Cocconi, Hart, Block, Harth, Fowler, Garrison, and Morris, *Phys. Rev.* **103**, 1493 (1956).

¹³W. A. Wallenmeyer, *Phys. Rev.* **105**, 1058 (1957).

SEARCH FOR THE REACTION $\mu^+ + e^- \rightarrow \gamma + \gamma^*$

C. M. York, C. O. Kim, and W. Kernan

Enrico Fermi Institute for Nuclear Studies and Physics Department, University of Chicago, Chicago, Illinois

(Received August 3, 1959)

One of the few reactions in which the direct interaction of two light fermions can be studied is the annihilation process

$$\mu^+ + e^- \rightarrow \gamma + \gamma^* \quad (1)$$

Furthermore, this reaction can be compared directly with the more familiar positron annihilation process.

In this experiment a beam of π^+ mesons is brought to rest in a $\frac{1}{4}$ -in.-thick disk of copper, as shown in Fig. 1. This disk is viewed by two,

5-in. diameter by $4\frac{1}{2}$ in. high, sodium iodide counters, I and II, through 2.8-in. diameter holes in lead collimators. The sodium iodide crystals are screened by 6-in. diameter scintillation counters, numbered 1 and 2, placed between the crystals and the exit face of the collimators.

Figure 2 is a block diagram of the electronic circuits used to select the reaction of Eq. (1). Fast pulses were obtained from the 5-in. duMont photomultiplier tubes used with the sodium iodide crystals, by means of a small inductance (about